RPE | Radiation Physics & Engineering
A Peer-Reviewed Journal
Published by K.N. Toosi University of Technology
http://rpe.kntu.ac.ir
Research Article

Radiation Physics and Engineering 2027; ?(?):?–?

Assessing the impact of boron distribution simplification on BNCT dosimetry

Fatemeh S. Rasouli*

Department of Physics, K.N. Toosi University of Technology, P.O. Box 15875-4416, Tehran, Iran

Accepted

HIGHLIGHTS

- Simplifying intratumoral boron distribution can affect BNCT dose calculations.
- Boron gradient direction influences the tumor dose distribution.
- Gradient orientation has a stronger impact at lower mean boron concentrations.
- Tumor AUC varies with the spatial arrangement of boron.
- Boron distribution affected BNCT dosimetry through both concentration and spatial arrangement.

ABSTRACT

Accurate dose calculation in boron neutron capture therapy (BNCT) requires an appropriate representation of intratumoral boron distribution. Although assuming a uniform boron concentration simplifies dosimetric modeling, the extent to which this approximation affects dose estimates under spatially heterogeneous conditions remains unclear. This study investigated the effects of intratumoral boron distribution on BNCT dosimetry using Monte Carlo simulations. A spherical tumor embedded in a Snyder head phantom was modeled with either a uniform boron concentration of 40 ppm or four concentric, equal-volume regions with heterogeneous concentrations. The heterogeneous models had mean tumor boron concentrations of 25, 30, and 35 ppm, with concentration gradients directed either from the tumor center toward its boundary or in the reverse direction. Depth-dose profiles, the area under the dose-depth curve (AUC) within the tumor, and the ratio of maximum tumor dose to maximum healthy-tissue dose were evaluated. Compared with the uniform 40-ppm reference, the heterogeneous models exhibited lower tumor-region AUC values, with reductions ranging from 5.94% to 41.17%. For a given mean boron concentration, the center-to-boundary configuration yielded a higher AUC than the boundary-to-center configuration. The relative AUC difference between these configurations decreased from 29.16% at a mean concentration of 25 ppm to 9.44% at 35 ppm. These findings demonstrate that the dosimetric impact of intratumoral boron distribution depends on both the mean boron concentration and its spatial arrangement, highlighting the importance of considering distribution patterns when simplifying boron uptake in BNCT dose calculations.

KEYWORDS

BNCT
Intratumoral boron distribution
Boron heterogeneity
Monte Carlo simulation
Dose calculation

HISTORY

Received:
Revised:
Accepted:
Published:

1 Introduction

Boron neutron capture therapy (BNCT) is a targeted radiotherapy modality in which the therapeutic effect results primarily from the nuclear reaction of ^{10}B with thermal neutrons, producing high-linear-energy-transfer (LET) alpha particles and lithium ions. Over the past decades, extensive research have investigated different aspects of BNCT, including neutron beam design and characterization, treatment planning, dosimetric methods, and the development of boron delivery agents to enhance boron accumulation in tumors while limiting toxicity to healthy tissues (Martın and Abrahantes, 2004; Torabi et al., 2013; Rasouli and Masoudi, 2015; Bavarnegin et al., 2016; Pistone et al., 2025; Kakino et al., 2024; Barth et al., 2005; Zamenhof et al., 1975). Among the factors influencing BNCT dosimetry, the boron concentration within the tumor and its spatial distribution are particularly important because they directly affect the spatial pattern of boron dose deposition (Conte et al., 2023; Teng et al., 2023).

*Corresponding author: rasouli@kntu.ac.ir

https://doi.org/

In practice, boron uptake is not necessarily homogeneous throughout a tumor, and heterogeneous boron distributions can produce spatial variations in the deposited dose. Recent studies incorporating heterogeneous boron distributions derived from ^{18}F-boronophenylalanine positron emission tomography (PET) have demonstrated differences in tumor dose distributions compared with conventional calculations based on uniform boron concentrations (Kobayashi et al., 2025). Moreover, Teng et al. (Teng et al., 2023) demonstrated that incorporating heterogeneous boron distribution, informed by PET imaging, is crucial for correcting dose-calculation errors and achieving more reliable estimates of tumor dose variations. Chen et al. (Chen et al., 2025), emphasized the implementation of open three-compartment pharmacokinetic models and advanced optimization algorithms to dynamically simulate boron distribution, thereby enhancing dose calculation accuracy and therapeutic efficacy. In particular, heterogeneous boron distributions may reveal low-dose regions within the tumor that may not be adequately represented when a homogeneous distribution is assumed. These findings highlight the importance of appropriately representing boron distribution in BNCT dose calculations.

Despite the recognized importance of boron heterogeneity, incorporating the actual spatial distribution of boron into BNCT dose calculations may not always be straightforward. Detailed boron distributions can be obtained from imaging techniques such as ^{18}F-boronophenylalanine positron emission tomography, but their incorporation into treatment-planning or Monte Carlo calculations requires additional data processing and spatial modeling. Moreover, the level of detail required to represent boron distribution accurately for dosimetric purposes is not yet clearly established. In Monte Carlo simulations, generally a homogeneous boron concentration is adopted as a practical simplification (Rasouli and Masoudi, 2015; Rahmani and Shahriari, 2011; Ganjeh and Masoudi, 2014), although this assumption neglects spatial variations in boron uptake. Conversely, representing the distribution with a large number of spatially varying concentration values may increase model complexity without necessarily providing a proportional improvement in dosimetric accuracy. Therefore, determining an appropriate level of simplification is an important issue for reliable and practical BNCT dose calculations.

Recent works have investigated the dosimetric effects of heterogeneous boron distributions using patient-specific imaging data, different boron concentrations, or time-dependent boron uptake Conte et al. (2023); Teng et al. (2023); Kobayashi et al. (2025); Chen et al. (2025). These studies have demonstrated that variations in boron concentration and its spatial distribution can affect the calculated dose within the target. However, to the best of our knowledge, it has not yet been clearly established whether the same effect is observed in simulation when the spatial distribution of boron is simplified, or what level of spatial detail is required for reliable dose estimation. In particular, it remains unclear whether a simplified representation of boron distribution can provide sufficiently accurate dosimetric results. Addressing this question could help identify an appropriate balance between the complexity of boron distribution modeling and the accuracy of BNCT dose calculations.

In the present study, we investigate the effect of simplifying the spatial distribution of boron on BNCT dose calculations using Monte Carlo simulations. A spherical tumor centrally located in a human head phantom is considered, and two representations of tumor boron distribution are compared. The first assumes a uniform boron concentration throughout the tumor, whereas the second represents the tumor using four concentric regions with distinct boron concentrations while maintaining a prescribed mean tumor concentration. By comparing these representations, we evaluate how the mean boron concentration, the spatial ordering of boron concentrations, and the resulting intratumoral gradients influence the calculated dose. The study provides a dosimetric assessment of the differences between homogeneous and simplified heterogeneous representations of intratumoral boron distribution under the conditions investigated.

2 Simulations

2.1 Phantom and Tumor Geometry

A Snyder head phantom was used to represent the human head geometry in the Monte Carlo simulations, including the major anatomical regions of the head such as the skin, bone, and brain, with a spherical tumor of 2.54 cm radius located at the center of the brain. The elemental compositions and densities assigned to the tissues of the phantom are summarized in Table 1. The same phantom and tumor geometry were used for all boron-distribution models considered in this study, allowing the dosimetric effects of boron spatial distribution to be evaluated without changes in the underlying anatomical geometry.

2.2 Neutron Source and Spectrum

The neutron source spectrum used in this study was taken from our previously designed beam shaping assembly based on a D-T neutron generator (Rasouli and Masoudi, 2012). The same neutron spectrum and source characteristics reported in the previous study were used without modification for all BNCT dosimetric calculations in the present work. This approach ensured consistency with the previously established source model while allowing the present study to focus on the effects of different spatial distributions of boron within the tumor.

2.3 Reference Model and Boron Concentration Assumptions

Based on reported boron concentrations associated with boronophenylalanine (BPA) administration Coderre et al. (1998), a boron concentration of 40 ppm in the tumor and a tumor-to-normal surrounding healthy tissue boron uptake ratio of 3.5:1 were considered in the simulations. The value of 40 ppm was defined as the upper limit of boron concentration within the tumor and was used as the reference concentration for the uniform tumor model. There-

Uncorrected Proof

Table 1: Elemental compositions of materials used in the simulated head phantom.

	Density	Weight percent (%)										
	($g.cm^{-3}$)	H	C	N	O	Na	P	Cl	K	S	Mg	Ca
Brain	1.04	10.7	14.5	2.2	71.2	0.2	0.4	0.3	0.3	0.2	-	-
Skull	1.61	5.0	21.2	4.0	43.5	0.1	8.1	-	-	0.3	0.2	17.6
Skin	1.09	1.0	20.4	4.2	64.5	0.2	0.1	0.3	0.1	0.2	-	-

fore, for the heterogeneous tumor models, 40 ppm was maintained as the maximum concentration, while lower concentrations were assigned to the remaining tumor regions according to the spatial distribution schemes described in the following sections. Thus, the heterogeneous models represent different spatial distributions and mean concentrations of boron within the tumor while maintaining the same maximum concentration.

2.3.1 Model 1: Uniform Boron Distribution

In the uniform model, the boron concentration was assumed to be spatially homogeneous throughout the tumor, with a concentration of 40 ppm assigned to the tumor volume. This model represents the reference condition in which no intratumoral variation in boron uptake is considered. The surrounding healthy tissue was assigned a boron concentration based on the tumor-to-normal tissue uptake ratio of 3.5:1.

2.3.2 Model 2: Four-Level Spatial Distribution

To investigate the effect of intratumoral boron heterogeneity, the tumor was divided into four concentric spherical regions with various boron concentrations. The radial boundaries of the four tumor regions were determined by dividing the total tumor volume into four equal-volume regions. Accordingly, the radius of the i-th boundary was calculated as

$$r_i = R\left(\frac{i}{4}\right)^{1/3}, \qquad i = 1, 2, 3, 4 \tag{1}$$

where $R = 2.54$ cm is the total tumor radius. This relation gives radial boundaries of $r_1 = 1.60$ cm, $r_2 = 2.016$ cm, $r_3 = 2.308$ cm, and $r_4 = 2.54$ cm. Thus, the four regions have equal volumes while forming concentric spherical layers.

Two concentration arrangements were considered: a center-to-boundary gradient, in which the boron concentration decreases from the innermost region toward the tumor boundary, and a boundary-to-center gradient, in which the concentration increases from the innermost region toward the boundary. In both arrangements, the four concentration levels were defined using an arithmetic sequence. Let C_1 and C_4 denote the concentrations in the innermost and outermost regions, respectively. For the center-to-boundary arrangement, the concentration in the innermost region was fixed at the maximum allowed value, $C_1 = 40$ ppm. The concentration levels were then defined as:

$$C_i = C_1 - (i-1)\Delta C, \qquad i = 1, 2, 3, 4 \tag{2}$$

where ΔC is the concentration difference between two successive regions. If $\overline{C}$ denotes the mean concentration across the four levels, then

$$\overline{C} = \frac{C_1 + C_2 + C_3 + C_4}{4} = C_1 - \frac{3}{2}\Delta C \tag{3}$$

Therefore, with $C_1 = 40$ ppm,

$$\Delta C = \frac{2}{3}(40 - \overline{C}) \tag{4}$$

and the concentration of the outermost region is

$$C_4 = 40 - 3\Delta C = 2\overline{C} - 40 \tag{5}$$

To ensure that the concentration in every tumor region remained at or above the prescribed minimum of 5 ppm, the condition $C_4 \geq 5$ was considered. This constraint yields a theoretical lower bound of $\overline{C} \geq 22.5$ ppm for the mean tumor boron concentration.

Based on the above formula, three heterogeneous concentration sets with mean tumor concentrations of 25, 30, and 35 ppm were considered. The corresponding concentration levels and constant gradient steps are summarized in Table 2. The 40-ppm case is also included as the uniform case, for which the gradient step is zero and all four regions have the same concentration. These concentration sets provide a uniform radial gradient while satisfying the prescribed upper and lower concentration limits and avoiding repeated concentration values. To examine the effect of the direction of spatial heterogeneity, each concentration set was considered in two arrangements: a center-to-boundary gradient, in which the concentration decreases radially outward, and a boundary-to-center gradient, obtained by reversing the order of the same four concentration levels.

For clarity, the six heterogeneous configurations are designated as models 2-(a) to 2-(f) throughout the remainder of this paper. Models 2-(a), 2-(c), and 2-(e) represent center-to-boundary concentration gradients with mean tumor boron concentrations of 25, 30, and 35 ppm, respectively. Models 2-(b), 2-(d), and 2-(f) represent the corresponding boundary-to-center gradients at the same mean concentrations.

Table 2: Boron concentration levels for the four-level spatial distribution model. The reported concentrations are in ppm.

$\overline{C}$	C_1	C_2	C_3	C_4	ΔC
25	40.00	30.00	20.00	10.00	10.00
30	40.00	33.33	26.67	20.00	6.67
35	40.00	36.67	33.33	30.00	3.33
40	40.00	40.00	40.00	40.00	0.00

Uncorrected Proof

Table 3: Normalized AUC values for the heterogeneous intratumoral boron-distribution models relative to the homogeneous reference model (Model 1, 40 ppm).

Model	Mean boron concentration (ppm)	Normalized AUC	Difference (%)
2-(a)	25	0.83	−16.96
2-(b)	25	0.59	−41.17
2-(c)	30	0.88	−11.60
2-(d)	30	0.72	−27.57
2-(e)	35	0.94	−5.94
2-(f)	35	0.85	−14.81
1	40	1.00	Reference

2.4 Dose Calculation and Tally Definition

The absorbed dose components were calculated separately using the MCNPX (version 2.6) F4 track-length tally. The resulting particle fluxes were converted to absorbed dose using the corresponding flux-to-dose conversion coefficients. The total biologically weighted dose was then calculated by combining the individual dose components as

$$D_{\mathrm{T}} = w_{\gamma} D_{\gamma} + w_{\mathrm{N}} D_{\mathrm{N}} + w_{\mathrm{fast}} D_{\mathrm{fast}} + \mathrm{CBE}.D_{\mathrm{B}} \quad (6)$$

where D_{γ}, D_{N}, D_{fast}, and D_{B} represent the absorbed-dose contributions from photons, thermal neutrons, fast neutrons, and the $^{10}\mathrm{B}(\mathrm{n},\alpha)^{7}\mathrm{Li}$ reaction, respectively. The radiation weighting factors were set to $w_{\gamma} = 1$ and $w_{\mathrm{N}} = w_{\mathrm{fast}} = 3.2$. The compound biological effectiveness (CBE) factor was applied only to the boron dose component and was assigned values of 1.3 for normal tissue and 3.8 for tumor tissue. For each simulation, 2×10^{8} particle histories were transported, resulting in statistical uncertainties below 1%.

The effects of boron-distribution simplification were evaluated using two complementary dosimetric parameters. First, the total biologically weighted dose was evaluated as a function of depth along the irradiation axis to obtain the depth-dose profiles for the different boron-distribution models. These profiles were compared to assess changes in the spatial distribution of dose resulting from the assumed intratumoral boron distribution. Second, the ratio of the maximum tumor dose to the maximum dose in the surrounding healthy tissue was calculated as

$$Q_{\mathrm{dose}} = \frac{D_{\mathrm{tumor,max}}}{D_{\mathrm{healthy,max}}} \quad (7)$$

where $D_{\mathrm{tumor,max}}$ and $D_{\mathrm{healthy,max}}$ denote the maximum total biologically weighted doses in the tumor and surrounding healthy tissue, respectively. This ratio was used to quantify the effect of boron-distribution simplification on the relative dose delivered to the tumor and healthy tissue.

3 Results and Discussion

The depth-dose profiles obtained for the uniform and heterogeneous boron-distribution models were compared to evaluate the effect of intratumoral boron distribution on the dose within the head phantom. The total biologically weighted dose was evaluated along the irradiation axis. For Model 2, three mean tumor boron concentrations of 25, 30, and 35 ppm were considered, with each concentration evaluated in both center-to-boundary and boundary-to-center gradient directions (See Table 2). The uniform 40-ppm distribution of Model 1 was used as the reference condition. The resulting depth-dose profiles for the six boron-distribution cases are presented in Fig. 1.

In all cases, the total dose exhibits a pronounced increase at the entrance to the tumor, followed by a progressive decrease with increasing depth. However, the total-dose profiles obtained using Model 2 differ from those of Model 1, with the magnitude and pattern of these differences varying among the examined cases. The discrepancies are particularly evident near the tumor entrance, where the dose gradients are steep, while the profiles tend to converge toward the deeper depths. This behavior indicates that replacing a homogeneous boron distribution with a spatially heterogeneous representation can alter the predicted depth-dose distribution, even when the overall tumor boron concentration is maintained. The boron-dose profiles in Model 2 also vary with depth, reflecting the spatial distribution of boron within the tumor. The differences between the boron-dose and total-dose profiles further demonstrate that the effect of boron redistribution should be evaluated in terms of both its specific dose contribution and its influence on the total dose. Overall, these results highlight the importance of accounting for intratumoral boron heterogeneity when assessing the depth-dependent dose distribution in BNCT.

To quantify the differences in dose profiles between the heterogeneous intratumoral boron-distribution models and the homogeneous reference model, the area under the dose-depth curve (AUC) was calculated over the tumor depth range. Numerical integration was performed using the trapezoidal rule, and the AUC for each model was normalized to that of Model 1. The resulting normalized AUC values are presented in Table 3.

All six heterogeneous models yielded lower depth-integrated doses than the homogeneous reference model. Among the center-to-boundary gradient models, the AUC ratio increased from 0.83 at a mean boron concentration of 25 ppm to 0.94 at 35 ppm. Similarly, for the boundary-to-center gradient models, the ratio increased from 0.59 to 0.85 over the same concentration range. For a given mean boron concentration, the center-to-boundary gradient produced a higher AUC than the corresponding boundary-to-center gradient. The smallest difference from the reference model was observed for model 2-(e), with a 35 ppm mean concentration and a center-to-boundary gradient, for which the integrated dose was 5.94% lower than that of Model 1. In contrast, model 2-(b), with a 25 ppm mean concentration and a boundary-to-center gradient, showed the largest difference, with a 41.17% reduction.

Figure 2 presents the depth-dependent percentage differences in total dose between the heterogeneous intratumoral boron-distribution models and the homogeneous reference model. Because the tumor was represented by

Uncorrected Proof

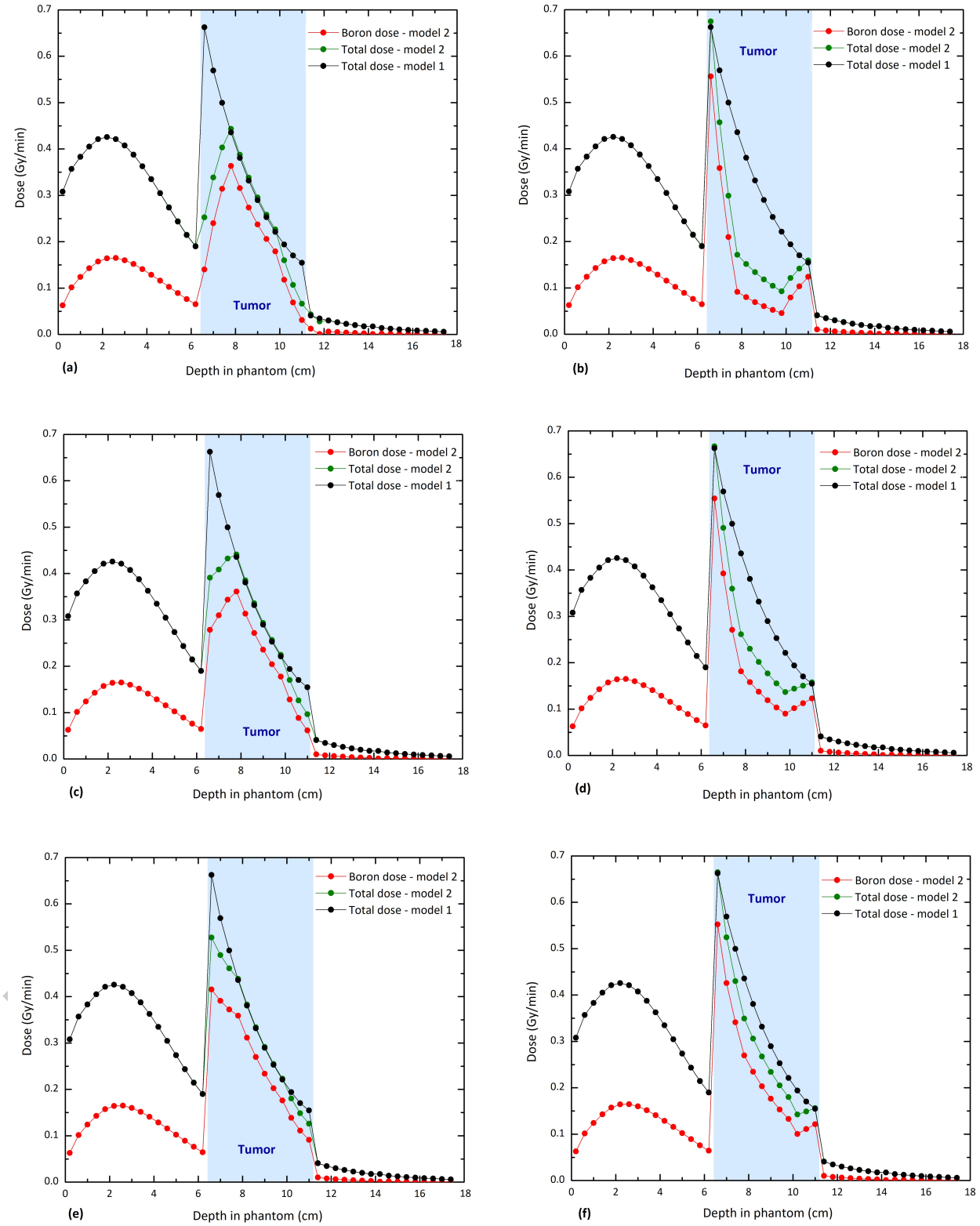

Figure 1: Depth-dose profiles comparing the six heterogeneous intratumoral boron-distribution models with the homogeneous reference model (Model 1): (a) 25 ppm mean tumor boron concentration with a center-to-boundary gradient, (b) 25 ppm with a boundary-to-center gradient, (c) 30 ppm with a center-to-boundary gradient, (d) 30 ppm with a boundary-to-center gradient, (e) 35 ppm with a center-to-boundary gradient, and (f) 35 ppm with a boundary-to-center gradient. Model 1 assumes a uniform tumor boron concentration of 40 ppm.

four concentric spherical layers, the dose differences were interpreted in relation to the boron concentration assigned to each layer and the direction of the concentration gradient. A clear dependence on the gradient direction was observed. For the center-to-boundary models of 2-(a), 2-(c), and 2-(e), the dose was substantially lower than the

Table 4: Comparison of AUC values for different mean boron concentrations and intratumoral boron distributions.

Mean boron concentration	Center-to-center	Boundary-to-boundary	Relative difference (%)
25 ppm	1.25	0.88	29.60
30 ppm	1.33	1.09	18.05
35 ppm	1.41	1.28	9.22

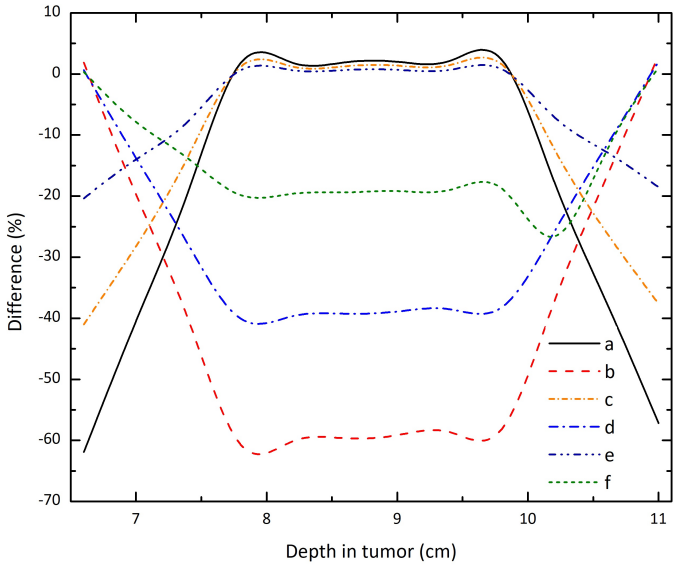

Figure 2: Depth-dependent percentage differences in dose relative to the homogeneous reference model (Model 1, 40 ppm) for the six heterogeneous intratumoral boron-distribution models: (a) 25 ppm, center-to-boundary gradient; (b) 25 ppm, boundary-to-center gradient; (c) 30 ppm, center-to-boundary gradient; (d) 30 ppm, boundary-to-center gradient; (e) 35 ppm, center-to-boundary gradient; and (f) 35 ppm, boundary-to-center gradient.

Uncorrected Proof

reference dose near the tumor entrance, with relative differences of -61.9%, -41%, and -20.4%, respectively, at a depth of 6.6 cm. These differences became progressively smaller toward the central region, where the boron concentration reached 40 ppm. Between depths of 7.8 and 9.8 cm, the relative differences were small and positive, ranging from approximately 0.6% to 2.3%. The same general behavior was observed for all three mean concentrations, although the magnitude of the differences depended on the concentration profile. In contrast, the boundary-to-center models 2-(b), 2-(d), and 2-(f) exhibited substantially lower doses in the central region, where the assigned boron concentrations were 40 ppm in the corresponding center-to-boundary models. Between depths of 7.8 and 9.8 cm, the relative differences ranged from approximately -58.26% to -60.7% for model 2-(b), from -38.2% to -40% for model 2-(d), and from -18.7% to -19.8% for model 2-(f). Toward the tumor boundary, the differences changed in accordance with the local boron concentration and the direction of the gradient.

Overall, the results demonstrate that the depth-dose response is sensitive to the spatial distribution of boron within the tumor. Reversing the concentration gradient produced distinct dose profiles, particularly in the central region. Nevertheless, because the heterogeneous models had mean boron concentrations of 25, 30, or 35 ppm, whereas the homogeneous reference model had a concentration of 40 ppm, these comparisons reflect the combined effects of the mean boron concentration and its spatial distribution. To quantify this effect within the tumor, the AUC was calculated over the tumor depth interval and compared between the center-to-boundary and boundary-to-center configurations for a given mean intratumoral boron concentrations of 25, 30, and 35 ppm.

As Table 4 presents, in all three cases, the center-to-boundary distribution yielded a higher AUC over the tumor region than the reverse distribution. The relative AUC difference decreased from 29.6% at 25 ppm to 18.05% at 30 ppm and 9.22% at 35 ppm. This progressive reduction suggests that the influence of distribution direction on the integrated dose response within the tumor diminished as the mean boron concentration increased over the investigated range.

To further compare the relative dose levels in the tumor and healthy tissue, the ratio of the maximum tumor dose to the maximum healthy-tissue dose, denoted by Q_{dose}, was evaluated for each boron-distribution configuration (Eq. (7)) . As summarized in Table 5, at mean boron concentrations of 25, 30, and 35 ppm, the boundary-to-center configurations yielded ratios of 1.58, 1.57, and 1.56, respectively, whereas the corresponding center-to-boundary configurations yielded ratios of 1.04, 1.03, and 1.24. Thus, the boundary-to-center configuration consistently resulted in a higher ratio than the corresponding center-to-boundary configuration at all three mean concentrations. Notably, the ratio for the boundary-to-center

Table 5: Ratio of maximum tumor dose to maximum healthy-tissue dose (Eq. (7)) for different intratumoral boron-distribution models.

Model	Mean boron concentration (ppm)	Boron distribution	Q_{dose}
2-(a)	25	Center-to-boundary	1.04
2-(b)	25	Boundary-to-center	1.58
2-(c)	30	Center-to-boundary	1.03
2-(d)	30	Boundary-to-center	1.57
2-(e)	35	Center-to-boundary	1.24
2-(f)	35	Boundary-to-center	1.56
1	40	Reference	1.55

configuration remained close to that of the homogeneous reference model (1.55). These findings highlight the importance of intratumoral boron distribution in determining the relative maximum-dose levels in the tumor and healthy tissue, beyond the effect of mean boron concentration alone.

Several limitations of this study should be acknowledged. First, the tumor was represented by a simple spherical geometry with four concentric regions of equal volume. Future studies could extend this framework to more realistic tumor geometries and more complex spatial boron distributions. Second, the heterogeneous configurations investigated in this study had different mean boron concentrations from the homogeneous reference. Therefore, the observed dose differences reflect the combined effects of mean boron concentration and spatial distribution. Strictly speaking, the observed dose differences cannot be attributed solely to the spatial arrangement of boron, as variations in the mean boron concentration also contribute to these differences. Further investigations using heterogeneous distributions with the same mean boron concentration would help isolate the effect of spatial arrangement on BNCT dosimetry. Finally, boron concentration in healthy tissues was assumed to be uniform, whereas actual boron uptake may also vary spatially in normal tissues. Incorporating heterogeneous boron distributions in both tumor and healthy tissues could provide a more comprehensive assessment of the dosimetric effects of boron distribution and improve the realism of BNCT dose calculations.

4 Conclusion

This study investigated the effect of intratumoral boron distribution on BNCT dosimetry using MCNPX simulations of a spherical tumor centered in a Snyder head phantom. A homogeneous boron distribution of 40 ppm was compared with heterogeneous four-layer configurations characterized by mean tumor boron concentrations of 25, 30, and 35 ppm, with boron concentration gradients directed either from the tumor center toward its boundary or in the opposite direction.

The results demonstrated that both the mean boron concentration and its spatial distribution influenced the calculated tumor dose. All heterogeneous configurations produced lower tumor depth-integrated doses than the homogeneous 40-ppm reference, although the magnitude of the reduction depended on the mean concentration and gradient direction. For a given mean concentration, the center-to-boundary configurations yielded higher depth-integrated doses than the corresponding boundary-to-center configurations. However, the difference between the two gradient directions decreased as the mean tumor boron concentration increased from 25 to 35 ppm, with the relative AUC difference decreasing from 29.6% to 9.22%.

The maximum tumor-to-healthy-tissue dose ratios further showed that the effect of boron distribution depends on the dosimetric endpoint considered. In particular, the ratios for the boundary-to-center configurations were similar to that of the homogeneous reference, despite differences in their depth-integrated tumor doses. Therefore, evaluating both dose metrics is necessary to better characterize the dosimetric impact of intratumoral boron heterogeneity.

Overall, these findings indicate that assuming a uniform intratumoral boron concentration can lead to differences in calculated BNCT dose estimates when the actual distribution is heterogeneous. The magnitude of these differences depends on both the mean boron concentration and its spatial arrangement. Accounting for intratumoral boron distribution may therefore be important for reliable BNCT dosimetry, particularly when boron concentrations are relatively low and spatial gradients are pronounced.

Conflict of Interest

The authors declare no potential conflict of interest regarding the publication of this work.

Funding

The authors declare that no funds, grants, or other financial support were received during the preparation of this manuscript.

References

Barth, R. F., Coderre, J. A., Vicente, M. G. H., et al. (2005). Boron neutron capture therapy of cancer: current status and future prospects. *Clinical Cancer Research*, 11(11):3987–4002.

Bavarnegin, E., Sadremomtaz, A., Khalafi, H., et al. (2016). Measurement and simulation of the TRR BNCT beam parameters. *Nuclear Instruments and Methods in Physics Research Section A: Accelerators, Spectrometers, Detectors and Associated Equipment*, 830:53–58.

Uncorrected Proof

Chen, Y., Zheng, Q., Wang, B., et al. (2025). Research on the dose calculation of BNCT based on the time-varying boron concentration in pharmacokinetics. *Journal of Radiation Research*, 66(6):627–637.

Coderre, J. A., Chanana, A. D., Joel, D. D., et al. (1998). Biodistribution of boronophenylalanine in patients with glioblastoma multiforme: boron concentration correlates with tumor cellularity. *Radiation Research*, 149(2):163–170.

Conte, V., Bianchi, A., and Selva, A. (2023). Boron neutron capture therapy: microdosimetry at different boron concentrations. *Applied Sciences*, 14(1):216.

Ganjeh, Z. A. and Masoudi, S. F. (2014). Neutron beam optimization based on a ^{7}Li(p,n)^{7}Be reaction for treatment of deep-seated brain tumors by BNCT. *Chinese Physics C*, 38(10):108203.

Kakino, R., Hu, N., Tanaka, H., et al. (2024). Out-of-field dosimetry using a validated PHITS model and computational phantom in clinical BNCT. *Medical Physics*, 51(2):1351–1363.

Kobayashi, Y., Nakamura, S., Takemori, M., et al. (2025). Comparison of dose distribution with and without reflecting heterogeneous boron distribution using 18F-BPA positron emission tomography in boron neutron capture therapy. *Applied Radiation and Isotopes*, 219:111720.

Martın, G. and Abrahantes, A. (2004). A conceptual design of a beam-shaping assembly for boron neutron capture therapy based on deuterium–tritium neutron generators. *Medical Physics*, 31(5):1116–1122.

Pistone, D., Bortolussi, S., Fatemi, S., et al. (2025). A GATE Monte Carlo study on ICRP110 phantoms for BNCT dosimetry evaluation. *Applied Radiation and Isotopes*, 220:111724.

Rahmani, F. and Shahriari, M. (2011). Beam shaping assembly optimization of Linac based BNCT and in-phantom depth dose distribution analysis of brain tumors for verification of a beam model. *Annals of Nuclear Energy*, 38(2-3):404–409.

Rasouli, F. S. and Masoudi, S. F. (2012). Design and optimization of a beam shaping assembly for BNCT based on D–T neutron generator and dose evaluation using a simulated head phantom. *Applied Radiation and Isotopes*, 70(12):2755–2762.

Rasouli, F. S. and Masoudi, S. F. (2015). A study on the optimum fast neutron flux for boron neutron capture therapy of deep-seated tumors. *Applied Radiation and Isotopes*, 96:45–51.

Teng, Y.-C., Chen, J., Zhong, W.-B., et al. (2023). Correcting for the heterogeneous boron distribution in a tumor for BNCT dose calculation. *Scientific Reports*, 13(1):15741.

Torabi, F., Masoudi, S. F., and Rahmani, F. (2013). Photoneutron production by a 25 MeV electron linac for BNCT application. *Annals of Nuclear Energy*, 54:192–196.

Zamenhof, R. G., Murray, B. W., Brownell, G. L., et al. (1975). Boron neutron capture therapy for the treatment of cerebral gliomas. I: Theoretical evaluation of the efficacy of various neutron beams. *Medical Physics*, 2(2):47–60.

Uncorrected Proof

©2027 by the journal.

RPE is licensed under a Creative Commons Attribution-NonCommercial 4.0 International License (CC BY-NC 4.0).

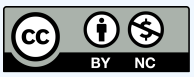



To cite this article:

F.S. Rasouli. Assessing the impact of boron distribution simplification on BNCT dosimetry. *Radiation Physics and Engineering*, In Press.

DOI:

To link to this article: